Biophysical Chemistry 252 (2019) 106191

Contents lists available at ScienceDirect

Biophysical Chemistry

journal homepage: www.elsevier.com/locate/biophyschem

Evaluation of heating effects on the morphology and membrane structure of *Escherichia coli* using electron paramagnetic resonance spectroscopy

Bade Tonyali[a], Austin McDaniel[a], Valentina Trinetta[a,b], Umut Yucel[a,b,*]

[a] Food Science Institute, Kansas State University, Manhattan, KS 66506, United States of America
[b] Animal Sciences and Industry, Kansas State University, Manhattan, KS 66506, United States of America

HIGHLIGHTS

- Structural changes in *E. coli* membrane with heating was studied with EPR.
- *E.coli* cell size increased from 2.3 to 3.0 μm when heated to 50 °C.
- Further heating caused shrinkage observed as decrease in size (ca. 1.7 μm).
- TEM was used to visualize the related morphological changes.
- Survival ability of bacteria is related to membrane and morphological changes.

GRAPHICAL ABSTRACT

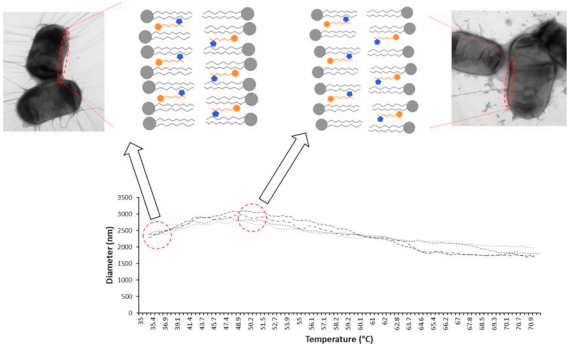

ARTICLE INFO

Keywords:
EPR spectroscopy
TEM
Dynamic light scattering
Heating
E. coli membrane, cell morphology

ABSTRACT

Bacterial cell characteristics, such as size, morphology, and membrane integrity, are affected by environmental conditions. Thermal treatment results in related structural changes, extent of which is determined by the microorganism's survival skills and inactivation kinetics. The objective of this study was to characterize changes in cell structure of *Escherichia coli* during heating using the combined analysis of dynamic light scattering (DLS), electron paramagnetic resonance (EPR) spectroscopy, and transmission electron microscopy (TEM) techniques. The size of *E. coli* cells increased from 2.3 μm to 3.0 μm with heating up to 50 °C followed by a shrinkage with further heating up to 70 °C. The morphological changes were verified using transmission electron microscopy. Related changes in membrane integrity was quantified via the mobility of 16-doxylstearic acid (16-DSA) spin probe using EPR spectroscopy. Two order parameters S_1 and S_2 defined on x- and y-axes, respectively, decreased with increasing temperature indicating loss of membrane integrity. The combined techniques as in this study can be used to further understand factors that play role in survival behavior of microorganisms.

1. Introduction

The survival kinetics of microorganisms is determined by the effects of external stresses, such as heat and antimicrobial compounds, on cell size, morphology, and membrane structure [1,2]. The extent of these changes is determined by inactivation mechanisms and the resistance of microorganisms to the applied stress. The heating process can damage multiple cellular elements, such as disruption of the peptidoglycan cell wall and damage to RNA, DNA, and enzymes. Microorganisms can resist thermal stresses by altering their cellular properties (i.e. adjustment

* Corresponding author at: Food Science Institute, Kansas State University, 1530 Mid-Campus Dr. North, Manhattan, KS 66056, United States of America.
E-mail address: yucel@ksu.edu (U. Yucel).

https://doi.org/10.1016/j.bpc.2019.106191
Received 12 March 2019; Received in revised form 20 May 2019; Accepted 22 May 2019
Available online 24 May 2019
0301-4622/

of lipid bilayer viscosity and rearrangement of the membrane layer to maintain the membrane functionality). However, cellular alterations can tolerate a maximum change, after which the cell structure irreversibly gets damaged [3].

The destruction of these elements interferes with the replication and the self-maintenance mechanisms of the cell. Moreover, changes such as the disengagement of the membrane from the cell wall, formation of pores, release of cell components out of the cell, and alterations in outer and inner cell membrane structures have been previously reported [4]. The increased cell membrane permeability, observed in parallel with increased membrane fluidity, disrupts the control over the transport mechanisms and eventually leads to the loss of internal homeostasis [5]. Indeed, it is know that this process results in compromised metabolic cell functions and leaching of the cell components [1,6]. Early studies measured particle size with microscopic methods, which require analysis of large number images and tedious sample preparation steps [7]. More recent studies commonly used flow cytometry to characterize membrane structure and mobility. This technique is based on use of fluorescence probes and the measurement is taken on each cell at a single time [8]. The changes in the membrane integrity under different stresses, such as temperature [4] and ultrasound [9], were previously investigated using this technique. In flow cytometry analysis, membrane integrity is characterized using dyes to stain specific components (e.g. DNA) in bacteria cell. The dying step requires time for permeabilization and washing steps afterwards which are challenging and time-consuming. Moreover, the cell aggregations might interfere with the sensitivity of measurements [10]. Recently, Vargas et al. showed the usability of dynamic light scattering (DLS) measurements to study the growth (i.e., size and population) of *E.coli* and *S.aureus* in the lag phase as an alternative to the traditional methods [11]. Electron Paramagnetic Resonance (EPR) spectroscopy is a non-destructive technique, which has been used to study membrane structures [1,3,12]. EPR spectroscopy is sensitive to the presence of molecules with unpaired electrons, where the spin relaxation of electrons is determined by the mobility of the molecules. In a spin-labeling technique, a stable free radical (i.e., spin probe) is introduced to the system and serves as a reporter molecule. The interaction between the spin probe and the target molecule, i.e. the cell membrane, is used for characterization studies. For example, a nitroxide radical with an aliphatic carbon chain aligns itself along the lipid bilayer, and the specific rotation on each axes is responsible for the shape of the complex slow-tumbling spectra [3,12,13]. The hyperfine splitting of slow-tumbling spectra is typically associated with the extent of rotational diffusivity of the spin probe on each axes [14].

Previously Glover et al. [1] used an aliphatic spin probe 5-doxylstearic acid (5-DSA) to characterize the membrane integrity of *Proteus mirabilis, Staphylococcus aureus,* and *Saccharomyces cerevisiae* under the action of surfactants. Similarly, other researchers used similar aliphatic spin probes to study the integrity and fluidity of human sperm plasma membranes [13], *Listeria monocytogenes* cell membranes [3], and bovine retina membranes [15] as a function of various external stresses. Therefore, we propose that EPR techniques can be used to characterize the changes in bacterial membrane, which eventually provides information for their survival ability. The objective of this study is to evaluate the effect of heating on the cell morphology and membrane mobility of *E. coli* by the combined analytical techniques of EPR, DLS, and transmission electron microscopy (TEM).

2. Materials and methods

2.1. Materials

Escherichia coli cultures (ATCC® 12435™) were obtained from American Type Culture Collection (ATCC®; Manassas, VA). The stock solutions were stored on Trypticase Soy Agar slants (TSA; Becton, Dickinson and Company, Sparks, MD) at 4 °C, and the cultures were grown in Tryptic Soy Broth (TSB; Becton, Dickinson and Company, Sparks, MD) prior to use. The spin probe, 16-doxylstearic acid (16-DSA; > 95.0% purity), was purchased from Enzo Life Sciences (NY, USA). Potassium chloride (KCl; Fisher Scientific, USA), peptone water (Bacto™ Peptone, Becton, Dickinson and Company, Sparks, MD) and phosphate-buffered saline (PBS; VWR International, LLC, Solon, OH) were analytical grade and used without any modification.

2.2. Growth curve

The cell count and absorbance measurements were performed following the method given in Fujikawa et al. [16] with some modifications. Briefly, an isolated colony of *E. coli* was inoculated into 10 mL of TSB and incubated at 35 °C overnight. 5 μL of the overnight (ca. 18 h) incubated cultures were transferred to 50 mL of TSB and kept at 35 °C. Every three hours, the optical density was measured using a UV–Vis spectrophotometer at 600 nm (Genesys, 10S UV–Vis, Thermo-Fisher). For *E. coli* enumeration, samples were serially diluted in 0.1% peptone water (Bacto™ Peptone, Becton, Dickinson and Company, Sparks, MD) and spread plated on TSA following the standard plate count agar method. All plates were incubated (VWR Incubator Gr Con 6, 85CF, Germany) at 35 °C for 24 h. Cell counts results were reported in logarithmic scale.

2.3. Particle size analysis

The particle size of *E. coli* cells was measured using a dynamic light scattering (DLS) instrument (DelsaMax Pro, Beckman Coulter, Brea, CA) based on the method described by Saini et al. [17] and Walker et al. [18] with modifications. Briefly, *E. coli* cells were grown in TSB at 35 °C until early stationary phase (ca. 9–12 h). The cell samples (5 mL) were centrifuged at 3800 rpm for 15 min (Allegra X-14R Centrifuge, Beckman Coulter) and resuspended in 5 mL of KCl solution (10 mM). The centrifugation and resuspension steps were repeated once. The twice rinsed cells were then diluted with 5 mL KCI solution to have a final concentration of 10^5–10^6 cells/mL. The effect of heating from 35 to 70 °C at a rate of 1 °C/min on cell size was studied using flow cell setup with the DLS instrument. The instrument operated at 45 mW with a wavelength of 532 nm. The average of five acquisitions of hydrodynamic diameter is reported for each measurement.

2.4. Membrane mobility analysis by EPR

The membrane mobility of *E. coli* cells were measured with EPR based on the method described by Glover et al. [1] with some modifications. Briefly, cell suspension in the early stationary phase (ca. 9–12 h at 35 °C) was centrifuged (3800 rpm for 15 min) and resuspended in glass vials containing fresh PBS (2.5 mL). Aliquots of 16-DSA solution (2.5 mM) was added to the cell suspension to have a final concentration of 400 μM. The cultures were incubated at 35 °C for 1 h to ensure 16-DSA partition into the membrane. Incubated cultures were heated to 42, 50, or 65 °C with gentle stirring in a hermetically sealed vial using a block heater (Heating/Stirring Module, Reacti-Therm III, Pierce). When the culture temperature was reached to set temperature (ca. 1 °C/min), the cell suspensions were centrifuged at 4300 rpm for 15 min and the supernatant was discarded. The cell pellets (ca. 50 mg) were transferred to borosilicate capillary tubes (VWR International, ID:0.5–0.6 mm) for EPR measurements. The EPR measurements were performed at room temperature in an EPR spectrometer operating at X-band (SpinscanX, ADANI, Belarus). The samples were analyzed under the following measurement conditions: center field 335 mT, sweep width 12 mT, modulation frequency 100 kHz, modulation amplitude 600 uT, microwave power 6 mW.

2.5. Transmission electron microscopy (TEM) analysis

TEM imaging of the *E. coli* cells were conducted in the Microscopy Facility, Division of Biology, at Kansas State University. The negative staining procedure was adapted from Trinetta et al. [19]. Briefly, post fixation of cells was carried out by 1% osmium tetroxide in 0.1 M cacodylate buffered solution. Cells were treated with ethanol, and propylene oxide, respectively. Thin sections were attached on copper grids and analyzed with a CM 100 TEM (Thermo Fisher Scientific). The images were captured with a Hamamatsu C8484 digital camera using an AMT digital image capture system (Chazy, NY).

2.6. Statistical analysis

The results were analyzed with analysis of variance (ANOVA) for significant of difference ($\alpha < 0.05$), and post-ANOVA calculations were performed using Tukey's multiple comparison test to evaluate differences between treatments by using Minitab software (v16, Minitab, Inc.).

3. Results and discussion

3.1. Cell size

DLS analysis is based on the movement of the scattered particles and measures the hydrodynamic diameter [11]. The hydrodynamic diameter is not actual size; however, this technique is reliable and allows direct and real-time monitoring in the characterization of the changes. Therefore, we hypothesize that this issue did not interfere with the results. The growth curve of *E. coli* at 35 °C was created using optical density measurements at 600 nm and microbial counts in Log CFU/ml (Fig. 1). The cells reached to stationary phase after 9 h of incubation with a 9-log population count. The cells at the early stationary phase were used for subsequent experiments as they are healthiest and most resistant to external stresses. We also monitored the size of *E. coli* cells during the different growth stages as hydrodynamic diameters using DLS technique. The *E. coli* cell size was ca. 2400 nm at the early stationary phase (Fig. 2). This is similar to previous data reported as measured by using optical microscopy [20,21]. The cell size effectively remained unchanged at the later stationary phase up to 24 h, however slightly but significantly ($p < .05$) larger size (ca. 3000 nm) was observed at the exponential growth phase. This is probably because the cell growth and cell division rates are increased, and therefore the number of large cells ready to divide is the highest in the exponential phase [22]. In contrast, the cells were in smaller size due to slower growth rate in the stationary phase.

In parallel to particle size measurements, the net surface charge of *E. coli* cells at their stern layer were also measured as zeta potential values, which largely remained unchanged at around −25 to −30 mV during growth. Other studies reported varying surface charge potentials (e.g., ca. between −60 and − 140 mV) of *E. coli* cells during the growth cycle [23,24]. However, the techniques used in these studies are completely different, such as impedance spectroscopy and intracellular microelectrodes. The stern later charge measured as zeta potential is affected by the ionic strength of the solution, and in our case the measurements were conducted after dispersing cells in KCl solution (10 mM), which resulting in lower surface charge potentials and eventually masking the fine differences that might be resulting from any compositional changes during growth.

The aliquots (170 μL) of *E. coli* cell suspensions were being heated from 35 to 70 °C at a rate of 1 °C/min in the flow chamber of the DLS instrument, and the cell diameter was automatically measured at 30 s intervals (Fig. 2). The cell size first gradually increased up to ca. 3000 nm until around 50 °C, followed by a decrease to ca. 2000 nm with further heating to 70 °C (Fig. 2). Similarly, Kim et al. [25] and Gabriel and Nakano [26] observed that inactivation of *E. coli* cells start around 50 °C. Mackey et al. [27] also indicated that membrane lipids melted around 40 °C and ribosomal subunits and soluble cytoplasmic proteins denatured irreversibly around 47 °C. After cell damage starts at temperatures above 50 °C, the cells lose their ability for homeostasis accompanied to disruption of membrane integrity and porosity. Therefore, continuing the heating results in reduction of the cell size likely due to leaching of cell components. The overall data for DLS measurement had high precision (standard deviations of our data were smaller than 10% from the mean values). The standard deviation was small and < 5% from the mean around the optimum growth temperature of the cells (37 °C). During heating, it increased; however, it was still under 10%. The small deviation from the mean indicated a good precision of the technique. In the next section, we investigated the changes in the membrane integrity and mobility using the EPR spectroscopy due to heating.

3.2. Membrane mobility analysis by EPR

The spin probe 16-DSA, produces an isotropic three-line spectra in solutions when it is not bound characteristic to fast tumbling spectra of nitroxide spin probes where hyperfine separations of parallel and perpendicular axes are averaged out [28–30]. The spin probe can penetrate into the bacterial membrane to provide structural information as illustrated in Fig. 3A. The fast-tumbling spectra of the 16-DSA in its

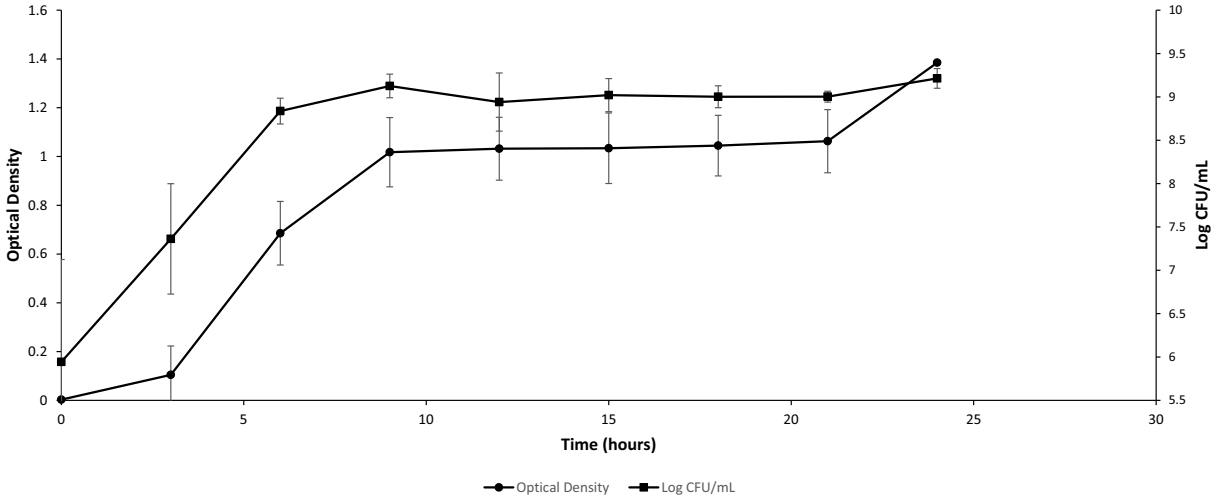

Fig. 1. Optical Density (O.D.) and log counts for *E. coli* cells grown at 35 °C.

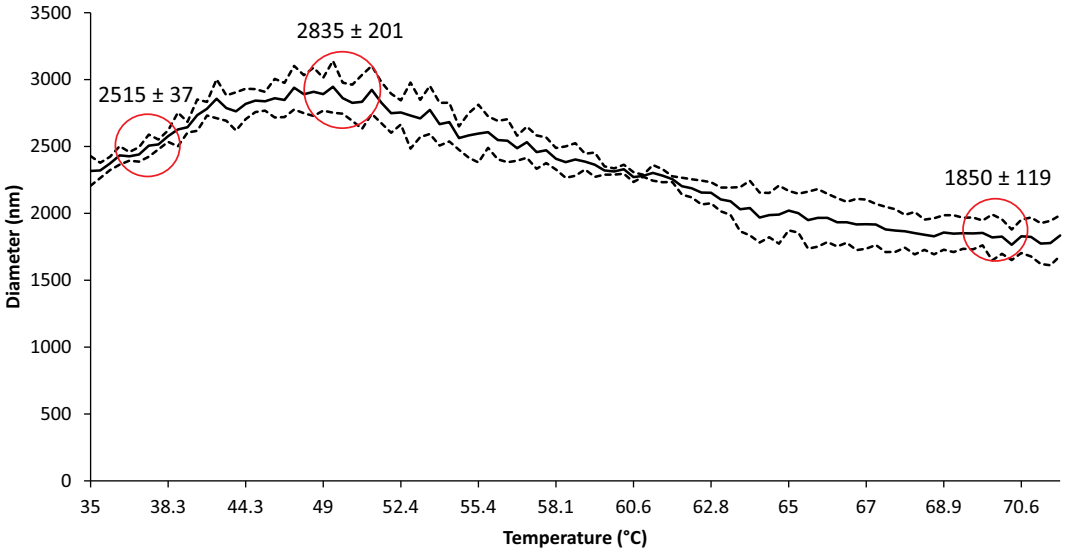

Fig. 2. Hydrodynamic diameter of *E. coli* cells with heat treatment (35–70 °C). The solid line represents the mean of individual particle size measurements (n = 4) and the dash lines represent ± standard deviations.

solution is a characteristic triplet signal for the nitroxide radical, where the rotation times on each molecular axes are averaged out (Fig. 4A). Once it is immobilized in the phospholipid membrane, it produces an anisotropic spectrum hyperfine splitting determined by spin relaxation times of individual molecular axes as shown in Fig. 4B. Some distortion in the spectra was observed in the form of spin exchange broadening related to probe localization at a certain spot [31].

The interaction between the spin probe and phospholipids causes distortion in the signal, and the shape of the EPR spectra was affected by heating due to changes in the mobility of the spin probe in interaction with the membrane. The spectra of the 35 °C indicate the control sample without heating. The change in the peak shape with heating is enhanced at the high-field region, where the position of the peak located around 339 mT showed decreasing hyperfine separation, while 337 mT diffused out with increasing temperature. The faster mobility of molecules with higher rotational diffusivities in parallel and perpendicular axes resulted in decreased spectral anisotropy. These changes were quantified by the order parameters S_1 and S_2 defined from the anisotropic hyperfine peaks associated with the two perpendicular axes [28,29,32]:

$$S_1 = (A_{zz}-A_{xx})/(A_{zz,max}-A_{xx,min}) \quad (1)$$

$$S_2 = (A_{zz}-A_{yy})/(A_{zz,max}-A_{yy,min}) \quad (2)$$

where A_{xx} is the hyperfine coupling constant related to motion on the x-axis, A_{yy} is the hyperfine coupling constant related to motion on the y-axis, A_{zz} is the hyperfine coupling constant related to motion on the parallel axis, and ($A_{zz,max}$ –$A_{xx,min}$) and ($A_{zz,max}$ –$A_{yy,min}$) are the hyperfine coupling constants for the rigid spectra. The measurements of hyperfine coupling constants were shown in Fig. 5. Rigid spectra values (2.73 and 2.78 mT for S_1 and S_2, respectively) are obtained under immobilized spin probe conditions in freeze-dried powders and in agreement with the literature [1,12,33].The order parameter is close to 0 in the fast tumbling spectra, while it is close to 1 in the slow tumbling spectra (i.e., when the spin probe is completely immobilized).

The Gram negative *E. coli* cells have two membranes separated by a thin cell wall. The outer membrane acts as a selective permeability barrier. The inner lipopolysaccharide layer is a selective barrier for small molecules and its rigid structure controls the passive diffusion of lipophilic compounds [34,35]. Although the spin-probe initially partitions to both inner and outer membrane, we assume that the spin probe is likely to wash-away from outer membrane with the double-rinse. Therefore, we expect the contributions coming from the outer membrane is expected to be small as compared to inner membrane, yet there is still probability that some small amount remains and contributes to the complex EPR spectra.

The order parameters S_1 and S_2 after heating to different temperatures were shown in Fig. 6. The lipid molecules exhibit molecular rotation (e.g. *gauche*-trans isomerization and lateral diffusion) along the parallel and perpendicular axes of carbon-carbon bond alkyl chain

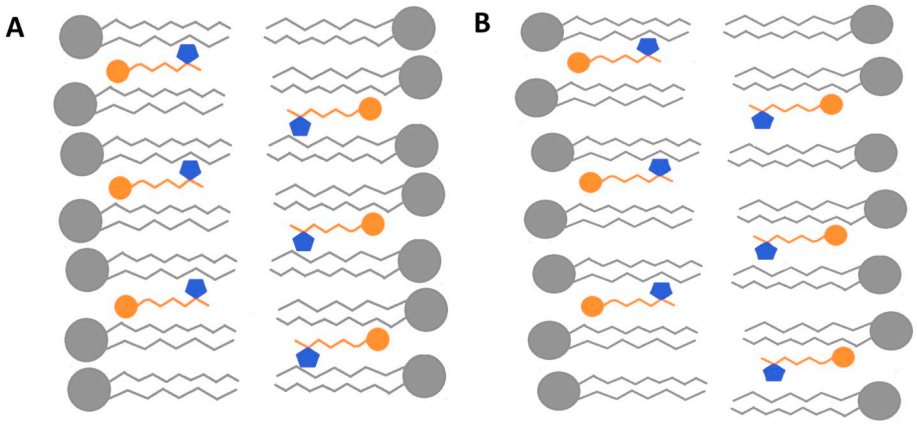

Fig. 3. The cartoon representation of alignment of spin probe 16-DSA (orange molecule) in the cell membrane A) at growth conditions, and B) after heating (not to the scale). The blue group on the spin probe represents the nitroxide group. (For interpretation of the references to colour in this figure legend, the reader is referred to the web version of this article.)

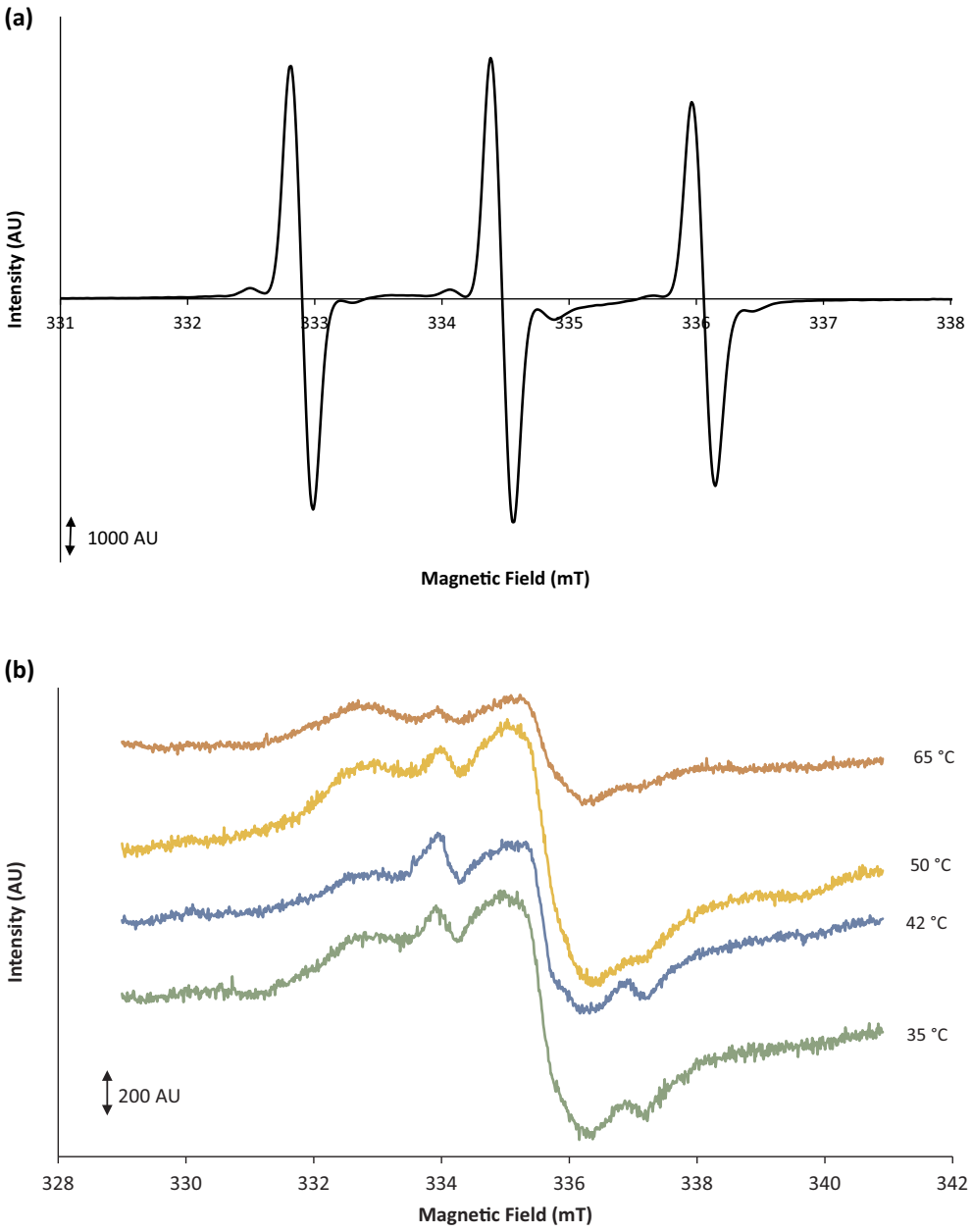

Fig. 4. EPR spectra of 16-DSA in A) PBS (400 uM solution) with the fast-tumbling spectra, and B) *E. coli* cells at 35, 42, 50, and 65 °C.

[32,36,37]. When the spin probe interacts with the cell membrane, the tail part (alkyl chain) continues rotational motion; however, the head structure (containing nitrogen moiety) is hindered by the membrane [32]. Therefore, the long axis of the tail part produces an anisotropic motion while the head structure governs a "wobbling" movement [32,38]. The motion direction of spin probe can be visualized as a cone shape. A rigid medium result in a smaller conical radius and motion amplitude to give a greater difference in hyperfine separations [31]. This restricted motion is reflected in the EPR spectra and order parameters.

The high magnitude of the order parameters at 35 °C indicate the control cells at the growth conditions where the spin probe is largely immobilized within the membrane. The motion of the spin probe molecule is largely restricted at the parallel axes aligned in the direction of bilayer structure of cell membrane, while it retains limited mobility at the x and y axes. The order parameter S_1 was significantly larger ($p < .05$) than S_2 probably related to the preferred alignment of the spin probe and the position nitroxide group within the membrane structure. The x-axis with the longer nitroxide dimension was freer to move between the phospholipids forming the bilayer, while the wobbling motion of the y-axis was more restricted with the peripheral fatty acid chains.

Both order parameters S_1 and S_2 decreased with increasing temperature indicating less restricted motion, and damage to membrane integrity. Similarly, Rottem et al. [14] showed that the outermost peaks in EPR spectra of DSA spin probes approached to each other (decrease in $2A_{zz}$ values) with less restricted motion in an investigation of mycoplasma membrane and effects of growth conditions. Moreover, Hubbell & McConnell [39] discussed the effect of temperature on the order parameter of aliphatic spin probes through phase transition of polymethylene chains of phospholipid membranes. When membranes heated above chain melting temperatures the order parameter abruptly changes indicating loss of membrane integrity. Similar observations was also reported by Mackey et al. [27] on melting of membrane lipids and changing structure of cell components. Therefore, we hypothesize that based on the thermal resistance of microorganisms are related to

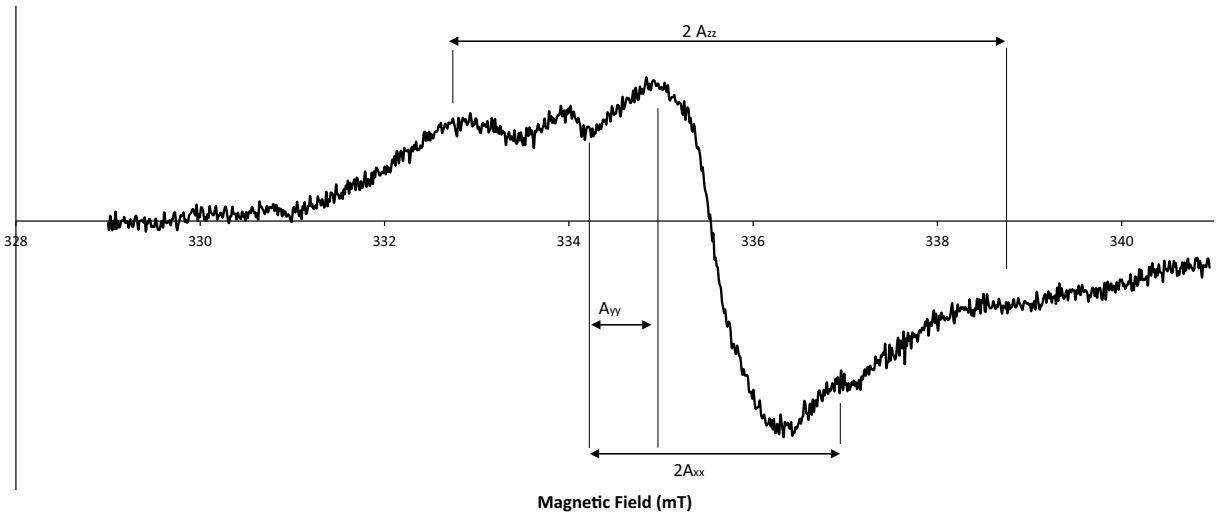

Fig. 5. Hyperfine coupling positions in the slow-tumbling EPR spectra.

the phospholipid composition of their cell membranes. The bacterial cells tolerate, survive, and finally go through adaptations under stress conditions, such as changing temperatures and the presence of essential oils or antibiotics. Other researchers studied the effect of stress conditions such as surfactant [1], essential oils [3], ultrasound [9], and the combination of ultrasound and antibiotics [40] on the cell membrane structure. Similar to our findings, these researchers related the loss of cell membrane integrity and disruption of tight packing to the phospholipid composition and structure.

The membrane integrity determines the cells ability for homeostasis, and a compromised membrane structure can result in dysfunction of the cell membrane activity and its selective permeability functionality. Baatout et al. [4] observed increased membrane permeability in *E. coli* cells submitted to 50, 60, and 70 °C temperature treatments and stated that an increase in membrane permeability was linked to damaged membrane integrity. The loss of membrane barrier functionality and increased permeability can eventually lead to leaching of cell components outside the cell to cause shrinkage. In the next section, we investigated the changes in cell morphology as a result of heating using TEM imaging.

3.3. Cell morphology analysis by TEM

The untreated (control) *E. coli* cells showed their characteristic rod shape morphology, and undamaged cell integrity with an intact membrane structure as shown in Fig. 7A1 and A2. The thin lines extended from the cells are the flagella. Heating the cells resulted in swelling (Fig. 7B1 and B2) as they reached to their largest size at around 50 °C characterized by DLS measurements. The thickness of the gap between the inner membrane and cell wall decreased compared to non-heated cells due to swelling (i.e., indicated with red circles in Fig. 7B). This enlargement compromised the cell membrane integrity as a result of two related phenomena: the increased mobility of the fatty acid chains and loss of lipoprotein structure with increasing temperature, and increased separation between molecules forming the membrane with enlargement. Similar observations were also reported by Munna et al. [41].

Further heating (up to 65 °C) caused the cells to shrink (Fig. 7C1 and C2). At this extreme point, the cell components leach out of the cell due to compromised cell membrane functionality. Without the internal resistance the membrane collapse observed as a much larger and irregular separation of the membrane from the cell wall (i.e., indicated with red circles in Fig. 7C). Similarly, Russell [42] reported that the severe damage to the inner membrane at high temperatures led to cell leakage and eventually to death. This was explained as the thermal degradation of inner membrane lipoproteins by high temperature. Baatout et al. [4] stated the bacterial cells undergo several changes such as membrane separation from the cell wall, pore formation, and leakage of cell

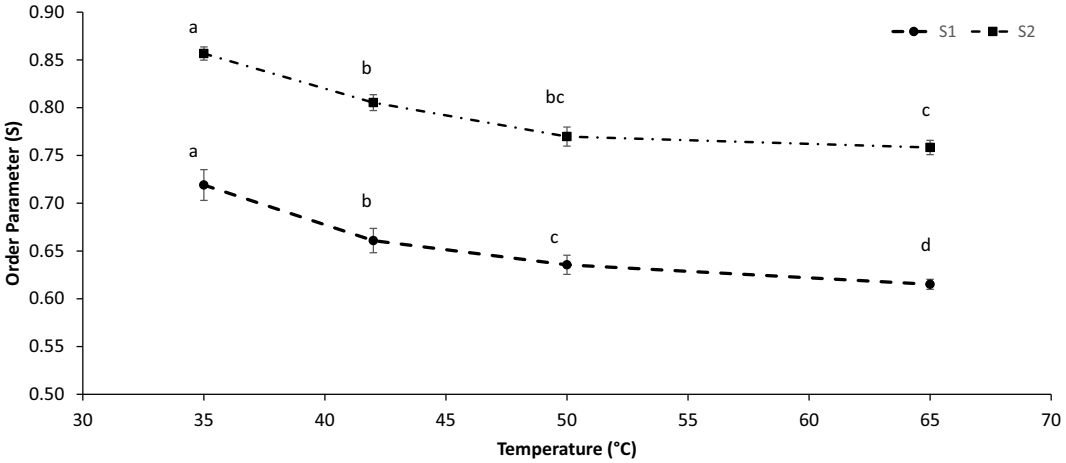

Fig. 6. The order parameters S_1 and S_2 calculated using eqs. 1 and 2, respectively. The different letters on the data indicate difference ($p < .05$) for the same parameters at different temperatures.

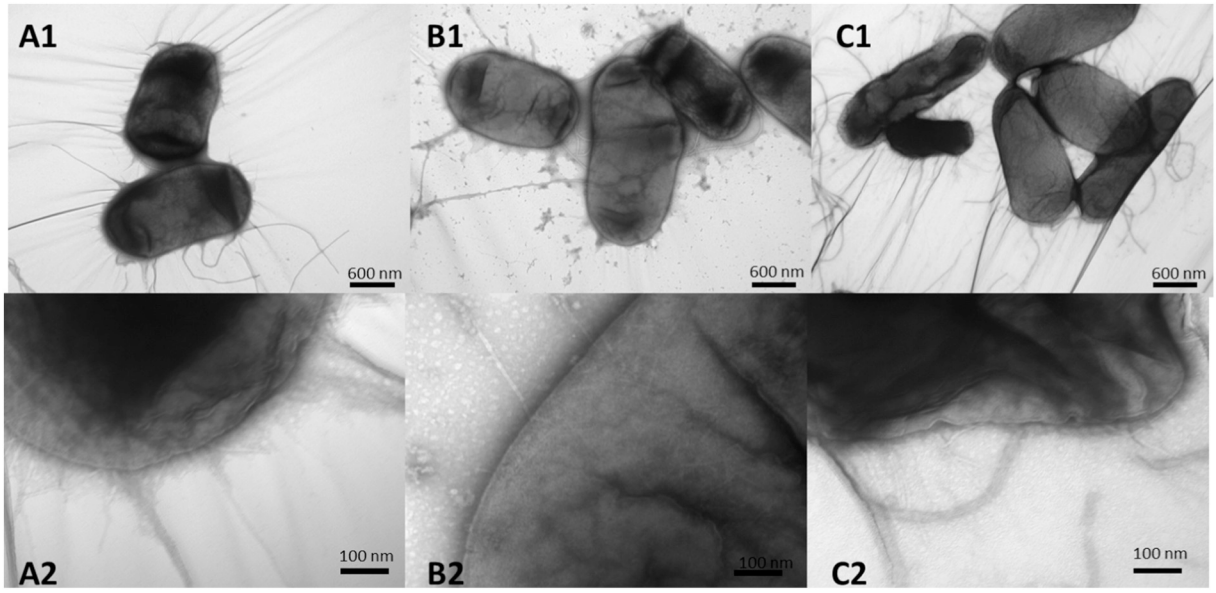

Fig. 7. TEM images of *E. coli* cells A) incubated at 35 °C, and heated to B) 50 °C, and C) 65 °C. The first row images are taken with x13,500 magnification; second row images are taken with x92,000 magnification.

components to the outer environment when they are exposed to temperatures higher than they can tolerate (e.g. 25 to 42 °C for *E. coli*). The swelling and shrinking of bacterial cells characterized with DLS and TEM analyses were in agreement with changes observed indicating changes in membrane integrity, which was consistently degraded with continuing heating as quantified by EPR measurements.

4. Conclusions

The present study showed that the EPR analysis (decreasing order parameter) in combination with DLS and TEM techniques showed the order of the changes in *E. coli* membrane integrity with temperature. This information can be used to compare the effects of environmental stresses that determine bacterial survival behavior. Our findings suggested the analysis of cell size, morphology, and membrane mobility can be used in parallel to provide a deeper understanding of structural changes related to bacterial thermal resistance. Multiple and related structural changes occur with external stresses, and their characterization is important to thoroughly understand survival skills of microorganisms. The combined approach proposed in this study can be helpful for further understanding of these changes that affect membrane integrity in combination with compositional information.

Acknowledgement

This work is supported by the USDA National Institute of Food and Agriculture, Hatch project 1014344. The authors thank Dr. Dan Boyle for his help on TEM analysis. Contribution no. 19-240-J from the Kansas Agricultural Experiment Station.

Declarations of interest

None.

References

[1] R.E. Glover, R.R. Smith, M.V. Jones, S.K. Jackson, C.C. Rowlands, An EPR investigation of surfactant action on bacterial membranes, FEMS Microbiol. Lett. 177 (1999) 57–62, https://doi.org/10.1016/S0378-1097(99)00289-X.

[2] G. Broeckx, D. Vandenheuvel, I.J.J. Claes, S. Lebeer, F. Kiekens, Drying techniques of probiotic bacteria as an important step towards the development of novel pharmabiotics, Int. J. Pharm. 505 (2016) 303–318, https://doi.org/10.1016/j.ijpharm.2016.04.002.

[3] A. Serio, M. Chiarini, E. Tettamanti, A. Paparella, Electronic paramagnetic resonance investigation of the activity of Origanum vulgare L. essential oil on the *Listeria monocytogenes* membrane, Lett. Appl. Microbiol. 51 (2010) 149–157, https://doi.org/10.1111/j.1472-765X.2010.02877.x.

[4] S. Baatout, P. De Boever, M. Mergeay, Temperature-induced changes in bacterial physiology as determined by flow cytometry, Ann. Microbiol. 55 (2005) 73–80.

[5] G. Cebrián, S. Condón, P. Mañas, Physiology of the inactivation of vegetative Bacteria by thermal treatments: mode of action, influence of environmental factors and inactivation kinetics, Foods 6 (2017) 107, https://doi.org/10.3390/foods6120107.

[6] N. Katsui, T. Tsuchido, R. Hiramatsu, M. Takano, I. Shibasaki, Heat-induced Blebbing and Vesiculation of the outer membrane of *Escherichia coli*, J. Bacteriol. 151 (1982) 1523–1531.

[7] F.J. Trueba, E.A. van Spronsen, J. Traas, C.L. Woldringh, Effects of temperature on the size and shape of Escherichia coli cells, Arch. Microbiol. 131 (1982) 235–240, https://doi.org/10.1007/BF00405885.

[8] E.A. Clementi, L.R. Marks, H. Roche-Håkansson, A.P. Håkansson, Monitoring changes in membrane polarity, membrane integrity, and intracellular ion concentrations in *Streptococcus pneumoniae* using fluorescent dyes, J. Vis. Exp. (2014) 1–8, https://doi.org/10.3791/51008.

[9] J. Li, J. Ahn, D. Liu, S. Chen, X. Ye, T. Ding, Evaluation of ultrasoundinduced damage to *Escherichia coli* and *Staphylococcus aureus* by flow cytometry and transmission electron microscopy, Appl. Environ. Microbiol. 82 (2016) 1828–1837, https://doi.org/10.1128/AEM.03080-15.

[10] M. Rieseberg, C. Kasper, K.F. Reardon, T. Scheper, Flow cytometry in biotechnology, Appl. Microbiol. Biotechnol. 56 (2001) 350–360, https://doi.org/10.1007/s002530100673.

[11] S. Vargas, B.E. Millán-Chiu, S.M. Arvizu-Medrano, A.M. Loske, R. Rodríguez, Dynamic light scattering: a fast and reliable method to analyze bacterial growth during the lag phase, J. Microbiol. Methods 137 (2017) 34–39, https://doi.org/10.1016/j.mimet.2017.04.004.

[12] L. Kong, U. Yucel, R. Yoksan, R.J. Elias, G.R. Ziegler, Characterization of amylose inclusion complexes using electron paramagnetic resonance spectroscopy, Food Hydrocoll. 82 (2018) 82–88, https://doi.org/10.1016/j.foodhyd.2018.03.050.

[13] M. Kveder, R. Rakoš, M. Gavella, V. Lipovac, G. Pifat, S. Pečar, M. Schara, EPR investigation of cell membrane fluidity upon external oxidative stimulus, Appl. Magn. Reson. 27 (2004) 77–86, https://doi.org/10.1007/BF03166303.

[14] S. Rottem, W.L. Hubbell, L. Hayflick, H.M. McConnell, Motion of fatty acid spin labels in the plasma membrane of mycoplasma, Biochim. Biophys. Acta Biomembr. 219 (1970) 104–113, https://doi.org/10.1016/0005-2736(70)90065-9.

[15] M. Duda, K. Kawula, A. Pawlak, T. Sarna, A. Wisniewska-Becker, EPR studies on the properties of model photoreceptor membranes made of natural and synthetic lipids, Cell Biochem. Biophys. 75 (2017) 433–442, https://doi.org/10.1007/s12013-017-0795-4.

[16] H. Fujikawa, A. Kai, S. Morozumi, A new logistic model for *Escherichia coli* growth at constant and dynamic temperatures, Food Microbiol. 21 (2004) 501–509, https://doi.org/10.1016/j.fm.2004.01.007.

[17] G. Saini, N. Nasholm, B.D. Wood, Implications of growth and starvation conditions in bacterial adhesion and transport, J. Adhes. Sci. Technol. 25 (2011) 2281–2297, https://doi.org/10.1163/016942411X574952.

[18] S.L. Walker, J.E. Hill, J.A. Redman, M. Elimelech, Influence of growth phase on adhesion kinetics of *Escherichia coli* D21g, Appl. Environ. Microbiol. 71 (2005)

3093–3099, https://doi.org/10.1128/AEM.71.6.3093.
[19] V. Trinetta, M. Rollini, S. Limbo, M. Manzoni, Influence of temperature and sakacin a concentration on survival of *Listeria innocua* cultures, Ann. Microbiol. 58 (2008) 633–639, https://doi.org/10.1007/BF03175568.
[20] I.Y. Galaev, M.B. Dainiak, F. Plieva, B. Mattiasson, Effect of matrix elasticity on affinity binding and release of bioparticles. Elution of bound cells by temperature-induced shrinkage of the smart macroporous hydrogel, Langmuir 23 (2007) 35–40, https://doi.org/10.1021/la061462e.
[21] G. Reshes, S. Vanounou, I. Fishov, M. Feingold, Cell shape dynamics in *Escherichia coli*, Biophys. J. 94 (2008) 251–264, https://doi.org/10.1529/biophysj.107.104398.
[22] T. Akerlund, K. Nordstrom, R. Bernander, Analysis of cell size and DNA content in exponentially growing and stationary-phase batch cultures of *Escherichia coli*, J. Bacteriol. 177 (1995) 6791–6797, https://doi.org/10.1128/jb.177.23.6791-6797.1995.
[23] H. Feile, J.S. Porter, C.L. Slayman, H.R. Kaback, Quantitative measurements of membrane potential in *Escherichia Coli*, Biochemistry 19 (1980) 3585–3590, https://doi.org/10.1021/bi00556a026.
[24] C.T. Bot, C. Prodan, Quantifying the membrane potential during *E. coli* growth stages, Biophys. Chem. 146 (2010) 133–137, https://doi.org/10.1016/j.bpc.2009.11.005.
[25] S.Y. Kim, H.G. Sagong, S.H. Choi, S. Ryu, D.H. Kang, Radio-frequency heating to inactivate Salmonella Typhimurium and *Escherichia coli* O157:H7 on black and red pepper spice, Int. J. Food Microbiol. 153 (2012) 171–175, https://doi.org/10.1016/j.ijfoodmicro.2011.11.004.
[26] A.A. Gabriel, H. Nakano, Inactivation of *Salmonella*, *E. coli* and *Listeria monocytogenes* in phosphate-buffered saline and apple juice by ultraviolet and heat treatments, Food Control 20 (2009) 443–446, https://doi.org/10.1016/j.foodcont.2008.08.008.
[27] B.M. Mackey, C.A. Miles, S.E. Parsons, D.A. Seymour, Thermal denaturation of whole cells and cell components of *Escherichia coli* examined by differential scanning calorimetry, J. Gen. Microbiol. 137 (1991) 2361–2374, https://doi.org/10.1099/00221287-137-10-2361.
[28] J. Seelig, Anisotropic motion in liquid crystalline structures, in: L.J. Berliner (Ed.), Spin Labeling, Academic Press, Inc, 1976, pp. 373–409, , https://doi.org/10.1016/B978-0-12-092350-2.50015-1.
[29] O.H. Griffith, P.C. Jost, Lipid spin labels in biological membranes, in: L.J. Berliner (Ed.), Spin Labeling, Academic Press, Inc, 1976, pp. 453–523, , https://doi.org/10.1016/b978-0-12-092350-2.50017-5.
[30] H.M. McConnell, Molecular motion in biological membranes, in: L.J. Berliner (Ed.), Spin Labeling, Academic Press, Inc, 1976, pp. 525–560.
[31] I.C.P. Smith, K.W. Butler, Oriented lipid systems as model membranes, in: L.J. Berliner (Ed.), Spin Labeling, Academic Press, Inc, 1976, pp. 411–451, , https://doi.org/10.1016/b978-0-12-092350-2.50016-3.
[32] W.K. Subczynski, J. Widomska, J.B. Feix, Physical properties of lipid bilayers from EPR spin labeling and their influence on chemical reactions in a membrane environment, Free Radic. Biol. Med. 46 (2009) 707–718, https://doi.org/10.1016/j.freeradbiomed.2008.11.024.
[33] J.H. Freed, Theory of slow tumbling ESR spectra for Nitroxides, in: L.J. Berliner (Ed.), Spin Labeling, Academic Press, Inc, 1976, pp. 53–132, , https://doi.org/10.1016/j.neurobiolaging.2011.12.002.
[34] H.I. Zgurskaya, C.A. López, S. Gnanakaran, Permeability barrier of gram-negative cell envelopes and approaches to bypass it, ACS Infect. Dis. 1 (2015) 512–522, https://doi.org/10.1021/acsinfecdis.5b00097.
[35] T.J. Silhavy, D. Kahne, S. Walker, The bacterial cell envelope, Cold Spring Harb. Perspect. Biol. 2 (2010) 1–16, https://doi.org/10.1101/cshperspect.a000414.
[36] G. van Meer, D.R. Voelker, G.W. Feigenson, Membrane lipids: where they are and how they behave, Nat. Rev. Mol. Cell Biol. 9 (2008) 112–124, https://doi.org/10.1038/nrm2330.
[37] K. Nakagawa, Diffusion coefficient and relaxation time of aliphatic spin probes in a unique triglyceride membrane, Langmuir 19 (2003) 5078–5082, https://doi.org/10.1021/la026813d.
[38] C. Sgherri, A. Porta, S. Castellano, C. Pinzino, M.F. Quartacci, L. Calucci, Effects of azole treatments on the physical properties of *Candida albicans* plasma membrane: a spin probe EPR study, Biochim. Biophys. Acta Biomembr. 1838 (2014) 465–473, https://doi.org/10.1016/j.bbamem.2013.10.015.
[39] W.L. Hubbell, H.M. McConnell, Molecular motion in spin-labeled phospholipids and membranes, J. Am. Chem. Soc. 93 (1971) 314–326.
[40] A.M. Rediske, B.L. Roeder, M.K. Brown, J.L. Nelson, R.L. Robison, D.O. Draper, G.B. Schaalje, R.A. Robison, W.G. Pitt, Ultrasonic enhancement of antibiotic action on *Escherichia coli* biofilms: an in vivo model, Antimicrob. Agents Chemother. 43 (1999) 1211–1214, https://doi.org/10.1128/AAC.43.5.1211.
[41] M.S. Munna, Z. Zeba, R. Noor, Influence of temperature on the growth of *Pseudomonas putida*, Stamford J. Microbiol. 5 (2016) 9, https://doi.org/10.3329/sjm.v5i1.26912.
[42] A.D. Russell, Lethal effects of heat on bacterial physiology and structure, Sci. Prog. 86 (2003) 115–137, https://doi.org/10.3184/003685003783238699.